Interference Mitigation and Decoding Through Gateway Diversity in LoRaWAN

Andrea Petroni and Mauro Biagi, *Senior Member, IEEE*

***Abstract*—Long Range (LoRa) represents an efficient low power solution for the Internet of Things. Specifically, LoRa defines a physical layer technology, while access control and network issues are handled by the LoRaWAN protocol. Channel access is essentially unslotted ALOHA, so LoRaWAN performance suffer from packet collision events. Such problem becomes more penalizing in dense network scenarios, where the large number of devices simultaneously connected makes the collision probability significantly grow. The largest part of solutions proposed to overcome LoRaWAN inefficiency is oriented to collision avoidance. Differently, we firstly present an algorithm for mitigating the interference among superposing LoRa signals, allowing collided packets to be detected anyway. Then, we propose a novel combining mechanism, implemented at the LoRaWAN network server, that exploits the information carried by the same packet, but received by different gateways, to achieve a more robust decoding. Hence, packet detection is reliably performed even in the presence of interference, thus reducing the need of retransmission and providing energy saving for end devices. Furthermore, simulation results show that the proposed solutions allow the end users to transmit exploiting low spreading factors, thus reducing the channel use that will be fundamental when dealing with larger scale network scenarios.**

***Index Terms*—LoRa, LoraWAN, cooperative decoding, interference cancellation, gateway diversity.**

I. Introduction

THE world of the Internet of Things (IoT) has been recently characterized by the spread Low Power Wide Area Networks (LPWANs) as a promising support to applications demanding for low energy consumption, low complexity but wide coverage area. Such requirements are typical of smart metering and monitoring activities where a large number of battery supplied devices/sensors transmit sporadically small-sized data. Several standards have been developed in the field of LPWANs, relying both on the Long Term Evolution framework, such as Narrowband-IoT, and on the unlicensed spectrum portion like Sigfox and LoRa [1]. Specifically, LoRa is a physical layer technology developed by Semtech [2] that defines a chirp spread spectrum (CSS) like modulation to enable long-range communication in the sub-Gigahertz unlicensed spectrum. LoRa devices interact by means of LoRaWAN, that is a medium access control (MAC) protocol which is however responsible for networking issues as well [3]. The LoRaWAN network topology is defined as *star of stars*, where the end devices (EDs) are connected to gateways (GWs) through a packet-oriented wireless communication based on LoRa signaling, while GWs are in turn linked to a remote network server (NS) via TCP/IP links. EDs uplink communication occurs following an unslotted ALOHA-like random access. Essentially, such strategy does not require any scheduling and resources pre-allocation, resulting as lightweight from the implementation point of view and, therefore, perfectly suited to LPWAN scenarios. On the other hand, as EDs transmission is not preceded by channel sensing, packet collisions may potentially occur and EDs are forced to spend additional energy for retransmission. Due to the sporadic and limited size traffic pattern generated by LoRa devices, packet collisions are considered as low probability events, making random access more computationally convenient than any other scheduling based method [4]. However, although at present this approach is still suitable, the ever growing deployment of IoT devices expected in the next years has put the problem of packet collision in LoRaWAN in the foreground, since the inefficiency of multiple access may impact on the devices lifetime as well [5].

The Authors are with the Department of Information Engineering, Electronics and Telecommunications (DIET), La Sapienza University of Rome, Via Eudossiana 18, 00184 Rome, Italy. Email: {andrea.petroni, mauro.biagi}@uniroma1.it

Manuscript received XXX XXX, 2021; revised XXX XXX, 2022.

A. Related works

Some works in the literature consider LoRaWAN traffic optimization as performed through adaptive allocation of the spreading factor (SF), representing a LoRa key parameter that defines the data rate and packet time length, so it essentially rules the channel occupancy for the transmitting ED. The authors in [6] propose a SF allocation technique aimed to maximize the packet success probability in an unslotted ALOHA massive multiple access scenario, providing also improvements in terms of connectivity. A different approach is proposed in [7] where SF allocation is performed not only as a function of the distance between ED and GW, but also considering the total number of connected devices. As LoRaWAN scalabity is mainly penalized by the inefficiency of the ALOHA random access, the largest part of the literature is devoted to the investigation of alternative MAC protocols fitting for massive multiple access scenarios. The work in [8] reports the analysis of slotted ALOHA and carrier-sense multiple access as potential candidates to replace unslotted ALOHA currently ruling LoRaWAN. In order to reduce the problem of collisions, the authors in [9] investigate the feasibility of listen-before-talk schemes to support LoRaWAN, showing that the achievement of robustness to collisions is paid in terms of protocol complexity growth and nodes energy consumption increase. A two-step lightweight protocol is proposed in [10] aiming to improve LoRaWAN

reliability and scalability through EDs transmit power and SF adaptation. The LoRaWAN scalability in dense network scenarios is also discussed in [11], where the LoRaWAN frame structure is conveniently reshaped to drive a MAC distributed-queuing algorithm for throughput enhancement. Overall, MAC protocols proposed for LoRaWAN efficiency improvement are essentially oriented to collision avoidance, that is the attempt to a priori prevent collisions. On the other hand, collision resolution based solutions have been only rarely considered in the literature. In this regard, it is worth noting that a LoRaWAN packet is physically represented by a LoRa signal. Therefore, addressing the interference among superposing LoRa signals may lead to resolve packet collision as well. The authors in [12] tackle the problem of collision resolution by exploiting the information about the time of arrival of different LoRa signals to perform the packets separation and decoding. However, the assumption about perfect packet synchronization at the GW considered by the authors oversimplifies the problem of interference cancellation. Actually, achieving time synchronization is not trivial [13], especially when dealing with overlapping signals. Another approach to collision resolution is described in [14], where successive interference cancellation (SIC) is proposed to separate two or more signals received with sufficiently different powers. This latter mechanism outperforms unslotted ALOHA regarding the probability of successful packet transmission, but its effectiveness is limited when the number of EDs simultaneously connected increases. In [15], the frequency offset caused by EDs radio hardware imperfections is exploited to handle the simultaneous reception of multiple packets, allowing the decoding of superposing signals. However, estimating the frequency offset from weak signals is not always reliable, and the presence of a large number of nodes makes the achievement of this task very challenging. Therefore, even detection performance may lower. The authors in [16] present a technique for decoding collided packets relying on the knowledge of LoRa signal time-frequency properties, so that the time misalignment between interfering symbols is used to resolve the collision. Finally, the work in [17] addresses the problem of both overlapping signals synchronization and decoding. Specifically, a two-step mechanism based on continuous signal dechirping is used for synchronization, while the time offset between overlapping packets is exploited for SIC and decoding. Performance are evaluated considering three LoRa signals, but the mechanism is claimed to be suited also to scenarios with a larger number of interfering packets.

Interestingly, the works mentioned above address the mitigation/cancellation of interference only by referring to signals received by a single reference GW. However, considering the broadcast nature of LoRa signaling, the packet transmitted by an ED can be received by multiple GWs. In this scenario, due to different propagation delays, the level of interference caused by other superposing LoRa signals can be different from GW to GW. This is the result of what we call gateway diversity, that can be fruitfully exploited to improve the separation and decoding of superposed LoRa packets. The use of spatial diversity is considered in [18], where the combining of signals received by multiple GWs is operated to improve the detection performance. By doing so, the effect of path attenuation is mitigated, allowing the detection of weak signals that may be not detectable by a single GW. However, such solution requires specific hardware and software capabilities not available for current LoRaWAN nodes.

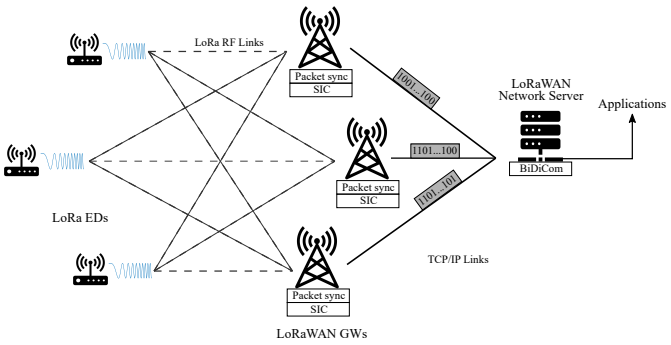

Fig. 1. LoRaWAN *star of stars* network topology.

B. Goal

Basing on the discussion reported above, we propose a twofold mechanism performing both the interference mitigation of superposed LoRa signals and, by exploiting gateway diversity, the achievement of a more reliable packet decoding. Specifically, our contribution presents:

- a synchronization mechanism for superposing LoRa packets. In this regard, we show how some properties of LoRa signaling can be fruitfully exploited to obtain a reliable channel estimation, to be further used for interference cancellation.
- an iterative SIC-based algorithm, implemented at GW side, responsible for the overlapping LoRa packets detection and separation.
- a novel cooperative decoding scheme based on gateway diversity, implemented at the NS, that combines the information given by multiple copies of the same packet retrieved independently by each GW to achieve more reliable decoding. Such technique is called Bit Diversity Combining (BiDiCom) as information combining is performed at bit level.
- the performance of the proposed solution as numerically evaluated considering realistic urban scenarios characterized by different GWs deployments.

A high level LoRaWAN network representation is depicted in Fig. 1, highlighting the proposed synchronization and SIC mechanisms as performed at GW side, while BiDiCom is implemented on the NS. To the best of our knowledge, gateway diversity for the decoding of colliding packets has never been considered before. Furthermore, the provided capability of decoding superposing signals *i)* reduces the need of packet retransmission and, therefore, the EDs energy consumption *ii)* allows the EDs to use low SF for transmission, thus reducing the channel usage time, *iii)* does not require changes in medium access control, so LoRaWAN saves the low complexity of unslotted ALOHA while benefiting from a higher robustness to packet collision.

This article has been accepted for publication in a future issue of this journal, but has not been fully edited. Content may change prior to final publication. Citation information: DOI 10.1109/TWC.2022.3172629, IEEE Transactions on Wireless Communications

The paper is organized as follows. In Sec. II we report an overview of the LoRaWAN protocol and LoRa signaling properties, together with the propagation model for single and multiple user case, respectively. Sec. III presents the algorithm for interference mitigation and packet detection. The mechanism for decoding based on gateway diversity is detailed in Sec. IV. Simulation results are reported and discussed in Sec. V. Finally, the conclusion is drawn in Sec. VI.

II. Overview of LoRa/LoRaWAN: system model

By following a top-down approach, in this section we detail the main LoRaWAN networking aspects at first and then we tackle the modeling of single link and multiple access characterizing LoRa modulation.

A. LoRaWAN network

While LoRa is the physical layer technology employed for wireless communication between ED and GW, LoRaWAN is the protocol for upper layers, responsible for the management of interactions involving all the network node types, that are EDs, GWs and a NS. In detail, the LoRaWAN network is organized in a *star of stars* topology (Fig. 1). Concerning the uplink, a LoRa packet is transmitted by the ED in an unslotted ALOHA-like fashion, exploiting radio bands specified region by region [19]. Each ED uses one of the available bandwidths, randomly selected so as to limit interference and collisions. In order to meet energy saving requirements, the transmit power of LoRa EDs is constrained to be 25 mW. Then, the collision-free packets received by a GW are decoded and forwarded to the NS by exploiting a reliable connection, either wired or wireless. The GW is also responsible for error detection and, possibly, correction. Due to the broadcast nature of the LoRa wireless channel, the same packet could be received by multiple GWs, so the NS operates deduplication allowing to save the most reliable packet copy and discard the other ones. Together with the decoded packet, each GW forwards to the NS information about the received signal quality, like signal-to-noise ratio (SNR) and received signal strength indicator (RSSI). Hence, in deduplication, the NS decides the packet copy to be saved as that one characterized by the highest SNR (or RSSI). Downlink is instead used only for those services requiring data-confirmed packets. In that case, if the integrity of the received packet is verified, the NS communicates back to the ED the acknowledgment using a GW as relay node, otherwise no feedback is sent. The EDs open specific time windows for the feedback reception, the length of which is defined by the device class, namely A, B and C [3]. The length of the receiving windows impacts on devices power consumption as well. If the ED does not receive any acknowledgment in that interval, then it automatically retransmits the packet. As depicted in Fig. 2, LoRaWAN considers the packet format as organized in two main parts [20]:

- a preamble, composed of typically 8 pilot symbols, 2 special symbols representing the synchronization word and a start-of-frame (SoF) delimiter given by 2.25 known symbols (thus meaning that the third symbol is truncated after 1/4 of its time duration). So, the resulting sequence is given by 12.25 symbols, employed for synchronization purposes.
- a payload carrying the frame information in form of header, data and a cyclic redundancy check (CRC). The header can be explicit or implicit. In the first case, it carries information about payload length, coding rate, and an additional CRC. In the latter case, such information is considered as fixed for the radio link, so it is not encoded in the frame.

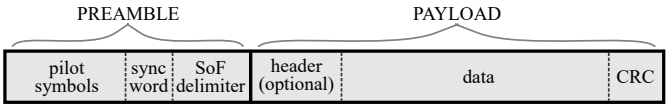

Fig. 2. LoRaWAN packet structure [20].

The LoRaWAN infrastructure is tailored to the IoT context, where network operations are required to be as simple as possible in order to limit the signaling and guaranteeing long lifetime to battery-supplied EDs. In this regard, the unslotted ALOHA principles ruling the channel access in LoRa perfectly match with the IoT energy efficiency requirements, since the sporadic nature of LoRaWAN traffic makes the problem of packet collision tolerable. However, in view of future larger scale networks due to the spread of IoT services, the effectiveness of the current LoRaWAN may be no more satisfactory, making the protocol rethinking necessary.

B. LoRa signaling: single link

As previously outlined, LoRa technology defines a particular signaling scheme derived from CSS modulation. So, the LoRa signal is modulated as a chirp, the frequency of which linearly changes within the interval ranging from f_{L} to f_{H} that corresponds to the signal bandwidth given as BW = f_{H}-f_{L}. The LoRa symbol time length is $T_s = 2^{\mathrm{SF}}/\mathrm{BW}$, with SF being the spreading factor. Basing on the SF, ranging from 7 to 12, and on BW, the bit rate R_b is [21]:

$$R_b = \frac{\mathrm{SF}\cdot\mathrm{CR}}{T_s} = \frac{\mathrm{SF}\cdot\mathrm{BW}\cdot\mathrm{CR}}{2^{\mathrm{SF}}} \tag{1}$$

with CR = $\frac{4}{5}, \frac{4}{6}, \frac{4}{7}, \frac{4}{8}$ being the coding rate. It is worth noting how SF rules the relationship between communication rate and range. In fact, given BW, T_s increases as SF grows, reducing R_b. Such behavior is typical of CSS techniques, where the reduction of bit rate and spectral efficiency brings benefits in terms of receiver sensitivity, allowing the communication range to be widened. As a peculiarity of LoRa modulation, signals transmitted over the same bandwidth but with different SFs are claimed to be orthogonal, even though such property is not always verified [22]. Tab. I reports further reference details, such as the typical LoRa packet size and time on air (ToA), that is the emission time.

The i-th LoRa symbol is defined from its starting frequency f_i, chosen among 2^{SF} discrete values corresponding to the number of symbols belonging the the modulation vocabulary, each one carrying SF bits. Specifically, we have that $f_i \in \mathcal{F} = \{f_i | f_{\mathrm{L}} \leq f_i \leq f_{\mathrm{H}}, f_i = f_{\mathrm{L}} + i\Delta f, \}$, with i=0,1,...,2^{SF}-1 and $\Delta f = 1/T_s$ being the discrete frequency shift

TABLE I
LoRa parameters for EU 863-970 MHz ISM band

SF	BW (kHz)	CR	R_b (bps)	Receiver sensitivity (dBm)	PHY Payload size min-max (bytes)	ToA min-max (ms)
12	125	4/6	244	-133.25	1-51	1155.1-2793.5
11	125	4/6	448	-134.50	1-51	659.5-1560.6
10	125	4/5	977	-132.75	1-51	288.8-698.4
9	125	4/5	1758	-131.25	1-115	164.9-676.9
8	125	4/5	3125	-127.25	1-222	82.4-655.9
7	125	4/5	5469	-126.50	1-222	46.3-368.9

step characterizing the LoRa chirp signal. Given T_s, the LoRa symbol can be seen as a sequence of 2^{SF} chips, the length of which is T_c = 1/BW. Each chip is associated to a frequency shift step Δf of the chirp signal. So, the i-th LoRa symbol waveform can be described in the time domain as [23]:

$$x_i^{(\text{UP})}(t) = e^{j2\pi[(i+t)\text{mod}(2^{\text{SF}})]\frac{t}{2^{\text{SF}}}} \quad \text{with } t = [0, T_s] \tag{2}$$

where the power of the chirp is normalized to 1. The signal in eq. (2) is defined as an *up-chirp*, since characterized by a linearly increasing frequency that shifts circularly between f_{L} and f_{H} as t increases. In fact, the i-th LoRa symbol starts with the frequency f_i that linearly grows up to f_{H}, then drops back to f_{L} and resumes to grow until the initial value f_i is reached. Differently from eq. (2), we have that a *down-chirp* signal, characterized by the linear decrease of frequency, is defined as $x_i^{(\text{DW})}(t) = \overline{x_i}^{(\text{UP})}(t)$, that is the complex conjugate of an up-chirp [23]. By recalling the LoRaWAN packet structure in Fig. 2, all the symbols belonging to both preamble and payload are up-chirps, except of the SoF delimiter that is composed of down-chirps. In the rest of the paper we refer to LoRa symbols as given by up-chirps, and we neglect the use of subscripts related to the chirp waveform in $x(t)$ so as to simplify the notation in the following.

LoRa signaling is used in the bi-directional communication between ED and GW. Concerning uplink, the i-th symbol received by the GW can be described as:

$$y(t) = x_i(t) * h(t) + w(t) \tag{3}$$

with $*$ being the convolution operator, $h(t)$ accounting for the effect of the channel and $w(t)$ representing a noise term modeled as a Gaussian random process with zero mean and σ_w^2 variance. In the most widespread approach in the literature, flat fading is assumed since the propagation effect can be considered as constant (in both the time and frequency domain) during the packet transmission by using Okumura-Hata and log-distance path loss model [24], [25].

The received information is retrieved from $y(t)$ through digital demodulation, that can be performed in a low complexity fashion (in place of conventional signals cross-correlation based method) by resorting to the so called *dechirping* [26]. Such technique consists in the following Hadamard product (indicated with the symbol $\circ$) applied to the chip-time sampled version of $y(t)$, indicated as $y[n]$:

$$y_{\text{DC}}[n] = y[n] \circ \overline{x}_{\text{ref}}[n] \tag{4}$$

where $\overline{x}_{\text{ref}}[n]$ is the complex conjugate of a reference symbol belonging to the LoRa vocabulary, typically $x_0[n]$. By taking into account the frequency circular shift property of LoRa signaling, eq. (4) returns $y_{\text{DC}}[n]$ as a single tone signal with carrier frequency that corresponds to the starting frequency of the transmitted symbol $x_i(t)$. Therefore, the decision on the received symbol is based on the recognition of the carrier frequency of $y_{\text{DC}}[n]$. In this direction, by computing the Discrete Fourier Transform (DFT) on eq. (4), we obtain $Y_{\text{DC}}[k]$ as a spectral characterization of $y_{\text{DC}}[n]$ returned at chip time, so that its 2^{SF} samples correspond to the 2^{SF} starting frequencies employable for LoRa signaling. The carrier frequency of $y_{\text{DC}}[n]$ is revealed by the highest magnitude bin in $|Y_{\text{DC}}[k]|$, so the decision on the received symbol is taken as:

$$\hat{i} = \underset{k \in \{0,1,\ldots,2^{\text{SF}}-1\}}{\text{argmax}} |Y_{\text{DC}}[k]| \tag{5}$$

where $\hat{i}$ represents not only the index of the highest magnitude bin in $|Y_{\text{DC}}[k]|$, but it also identifies the index of the starting frequency index related to the received LoRa symbol $y[n]$ (and, if the decision is correct, to the transmitted x_i, with $i = \hat{i}$).

Dechirping is used for LoRa signal demodulation, so it can be applied to decode LoRaWAN packets since essentially given by a sequence of LoRa symbols. In order to clarify the terminology used in the rest of the paper, we refer to LoRa symbols when dealing with the processing of physical signals, while we refer to LoRa packets when dealing with LoRaWAN access and networking issues.

C. LoRa signaling: multiple users

The problem of packet collision in LoRaWAN is a direct result of the interference arising at the physical layer when multiple signals overlap at the receiver. So, being able to reliably separate LoRa signals entails the network capability to resolve packet collision. In this regard, let us highlight that the processing of signals in the current LoRa/LoRaWAN implementation is typically performed assuming an interference-free scenario, as modeled in eq. (3). So, by referring to dechirping-based demodulation, the reliability of eq. (5) depends uniquely on the SNR (and, of course, on the accuracy of synchronization). Such aspect can be appreciated by referring to some examples reported in Fig. 3 where, by considering the transmission of the symbol $x_i(t)$, with i=32 and SF=7, it is shown the DFT of a dechirped LoRa symbol $|Y_{\text{DC}}[k]|$ at the receiver. Fig. 3(a) describes the case of high SNR where the carrier frequency of the dechirped signal is easily detectable as there is only a single component in $|Y_{\text{DC}}[k]|$ significantly higher than the others. So, the decision on the received symbol according to eq. (5) is extremely reliable ($\hat{i}$=32 in the example). On the other hand, when dealing with low SNR as referred in Fig. 3(b), the received signal is strongly corrupted by noise and the detection of the carrier frequency component becomes very difficult. In fact, the amplitude of bins in $|Y_{\text{DC}}[k]|$ results quite uniform, and errors may occur when trying to recognize the correct peak ($\hat{i}$=23 in place of $\hat{i}$=32). In order to provide a further example, let us consider now the presence of two EDs, namely u_1 and u_2, transmitting with the same SF their respective symbols $x_i^{(u_1)}$ and $x_j^{(u_2)}$ ($i \neq j$) that reach simultaneously the same reference GW.

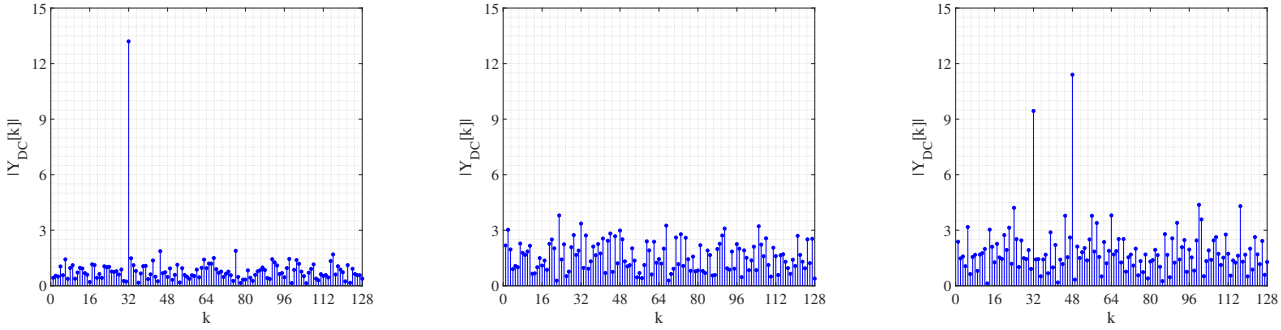

(a) High SNR (b) Low SNR (c) 2 symbols overlapping

Fig. 3. Graphical examples of symbols demodulation in different scenarios, considering SF = 7.

We assume the absence of interference due to other EDs transmitting with different SFs, thus meaning that in general we consider the SFs as orthogonal [23]. As the received signal results from the overlapping of the two symbols, eq. (3) can be rewritten as:

$$y(t) = x_i^{(u_1)}(t) * h_{u_1}(t) + x_j^{(u_2)}(t) * h_{u_2}(t) + w(t) \quad (6)$$

where $h_{u_1}(t)$ and $h_{u_2}(t)$ model the propagation of the signals emitted by u_1 and u_2, respectively. By assuming $h_{u_1}(t)$ and $h_{u_2}(t)$ as introducing sufficiently low signal attenuation with respect to the noise level, the dechirping of $y(t)$ reveals the presence of two main frequency components, represented by two peaks in the corresponding $|Y_{\text{DC}}|$ shown in Fig. 3(c). In this case, the received symbols would be correctly decoded since the position of such peaks in $|Y_{\text{DC}}|$ can be clearly identified, however it is not possible to recognize reliably which is the ED that each symbol has been transmitted from. So, it follows that now the reliability of the detection depends not only on the SNR of each signal, but also on the power difference between the received symbols. In fact, the probability of mistaking the decision on the received symbol grows as the magnitude of the peaks in $|Y_{\text{DC}}|$ becomes comparable, and this depends on $h_{u_1}(t)$ and $h_{u_2}(t)$ since the power of the transmitted symbols is the same. Furthermore, another issue rising from the superposition of two or more symbols is the so called *capture effect* [14]. This phenomenon occurs when two or more signals arrive at the receiver superposed in time, but only the strongest one can be detected, while the others suffer from shadowing that causes misdetection. The concept of capture effect can be extended from symbols to LoRa packets overlapping. In that case, the strongest packet is detected, while the weaker ones are lost leading to the need of their retransmission. Starting from the problem of decoding superposed symbols, we introduce now a more generalized scenario referring to the overlap of different LoRa packets collected by a single GW. We mentioned earlier that the LoRa packet emitted by the u-th ED is characterized by a preamble field and a payload one, hence by considering the possible analytical representation we have the sum of two non overlapping signals (since they are separated in time) as:

$$p_u(t) = z(t) + q_u(t) \quad (7)$$

where $z(t)$ and $q_u(t)$ describe the transmitted preamble and payload, respectively. Hence, given the presence of U EDs transmitting a packet each, the overall signal collected by the receiving GW is expressed as the sum of U packets *potentially* overlapping:

$$y(t) = \sum_{u=1}^{U} p_u(t - T_e^{(u)}) * h_u(t) + w(t) \quad (8)$$

with $T_e^{(u)}$ being the emission time of the u-th ED packet. In fact, the interference among signals depends on the time difference of arrival of packets, that may lead to problems of synchronization and decoding. In this latter case, interference among signals results in the packet collision event.

III. Packet Detection at the Single Gateway

Basing on eq. (8), the problem of LoRa packets collision can be addressed as the overlap of different LoRa signals at the receiving GW. The problem of interference arises when multiple EDs transmit with the same SF over the same bandwidth. So, the correct separation of LoRa packets entails two fundamental tasks to be accomplished, that are synchronization and decoding. In this direction, we introduce a SIC-based algorithm allowing the achievement of these goals.

By assuming the GW as performing signal sampling at chip time, we define the length of each LoRa packet $L_{\text{p}} = L_{\text{z}} + L_{\text{q}}$ samples, L_{z} and L_{q} being the length of the preamble and the payload, respectively. Moreover, the length of $y[n]$ is equal to L_{y} that can be at maximum $U \cdot L_{\text{p}}$ long so to let a single GW collect U LoRa packets coming from U different EDs, as described in eq. (8). As further detailed, the proposed mechanism proceeds with interference cancellation being performed recursively. In this regard, we refer to $y[n]^{(s)}$ as the signal received at the single GW in correspondence of the s-th SIC iteration, thus meaning that $y[n]^{(0)} = y[n]$. As a general comment, we want to anticipate here that if we are able to decode all the U packets in $y[n]$, at the end SIC will be characterized by s=U iterations. The flowchart in Fig. 4 summarizes the algorithm steps, organized in gray boxes.

A. LoRa signals synchronization

The first concern to be addressed for packet detection is synchronization, that is the recognition of the packet time of

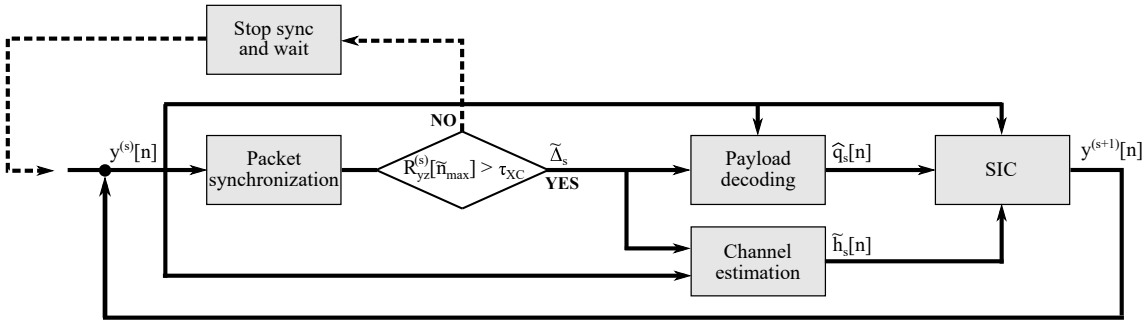

Fig. 4. Block scheme describing the proposed packet detection mechanism.

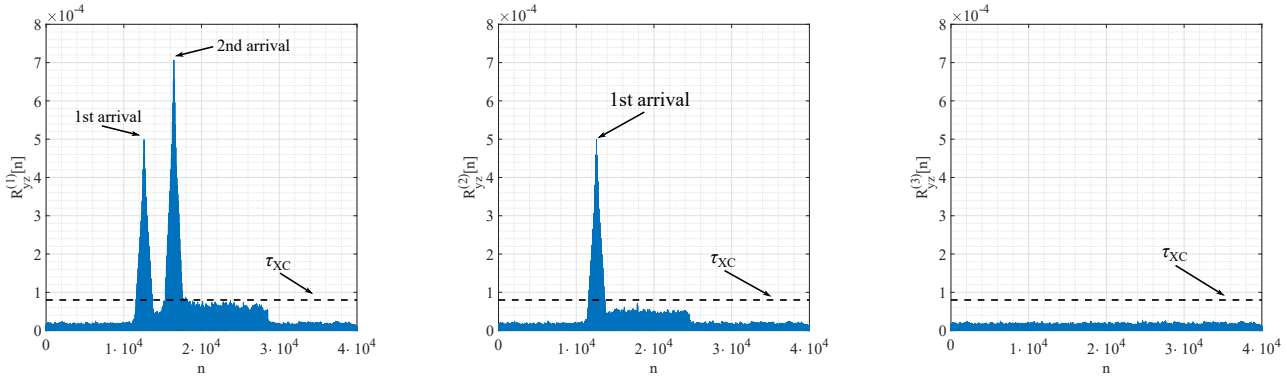

(a) Iteration $s = 1$ (b) Iteration $s = 2$ (c) Iteration $s = 3$

Fig. 5. Graphical example of the proposed interference cancellation when 2 LoRa packets overlap at the receiving GW.

arrival. By exploiting the knowledge of the packet preamble, referred as $z_{\text{ref}}[n]$ and previously mentioned, synchronization can be achieved starting from the expression:

$$R_{yz}^{(s)}[n] = |y^{(s)}[n] \circledast z_{\text{ref}}[n]| \tag{9}$$

where $R_{yz}^{(s)}[n]$ results from the modulus of the cross-correlation between $y^{(s)}[n]$ and $z_{\text{ref}}[n]$, denoted by the operator $\circledast$, obtained at the generic s-th algorithm iteration. Interestingly, the potential arrival of LoRa packets can be revealed by the presence of peaks in $R_{yz}^{(s)}[n]$. So, the absolute value operation is considered in eq. (9) achieve the synchronization through the recognition of local maxima in $R_{yz}^{(s)}[n]$. Furthermore, by recalling eq. (8), the amplitude of the peak associated to the arrival of the u-th packet is function of channel impulse response described by $h_u(t)$, hence the highest the peak is, the strongest the power of the corresponding received packet is. A graphical example of $R_{yz}^{(s)}[n]$ is reported in Fig. 5(a), where it is possible to observe two peaks referring to two LoRa packets received by the GW at different times. In general, the s-th iteration of the proposed algorithm concerns the search for the highest peak in $R_{yz}^{(s)}[n]$ providing the synchronization with strongest packet gathered in $y^{(s)}[n]$, to be further decoded and separated from the other received packets. It is worth noting that, following the proposed approach, the received packets are detected in descending order of power (measured for synchronization) that, in general, may not correspond to the order of arrival, as shown in Fig. 5(a). Basing on the cross-correlation properties, the length of $R_{yz}^{(s)}[n]$ is L_{yz}=2 $\cdot$ max($L_{\text{y}}, L_{\text{z}}$)-1. So, given $\tilde{n}_{\text{max}}$ as the index of the highest valued sample in $R_{yz}^{(s)}[n]$:

$$\tilde{n}_{\text{max}} = \underset{n\in[0,L_{\text{yz}}-1]}{\text{argmax}} \; R_{yz}^{(s)}[n] \tag{10}$$

we obtain $\tilde{\Delta}_s$ as:

$$\tilde{\Delta}_s = \tilde{n}_{\text{max}} - \left\lceil \frac{L_{\text{yz}}}{2} \right\rceil + 1, \tag{11}$$

representing the estimate of time of arrival of the strongest signal component at iteration s. Seeking for the maximum can lead to find the user packet exhibiting the highest power level. However this is not a guarantee that the maximum is sufficiently high, hence we choose to consider a threshold value τ_{XC} that has a twofold role. First, it is used to ascertain that we are considering something that is not below the receiver sensitivity level. Second, if $R_{yz}^{(s)}[n]$ is beyond the threshold, we recognize the presence of a packet to be detected. On the other hand, if $R_{yz}^{(s)}[\tilde{n}_{\text{max}}] < \tau_{\text{XC}}$, it is likely that no other user packets are present, and GW waits for another signal window to be processed. It is worth noting that the achievement of synchronization with the s-th packet allows the algorithm to continue with the decoding of the payload symbols in parallel with channel estimation. Finally, the accomplishment of the last mentioned two tasks allows SIC to be performed.

B. Channel estimation and detection

As previously mentioned, channel estimation and detection can be performed in parallel. In this regard, we recall from Sec.

II-B that dechirping represents a reliable and low complexity method for signal demodulation, with eq. (5) returning the index of the decided symbol. Furthermore, it is worth noting that, since the transmit power of EDs is fixed and known, the spectral analysis of the received signal may also reveal information about the channel effect. Typically, channel estimation is performed on some known pilot symbols. In the LoRa case, the sequence of symbols composing the packet preamble can be conveniently exploited to accomplish this task. Specifically, let us consider $x_0[n]$ as the known signal waveform from eq. (2), describing the pilot symbols of the packet preamble. Once achieved the symbol synchronization, the signal obtained after dechirping is a pure single tone. The corresponding spectral representation $Y_{\mathrm{DC}}[k]$ presents the bin with index 0 as high valued since representing the signal component around the frequency $f_0 \equiv f_L$. The amplitude of the other bins instead depends on the noise level and is in general low for high SNR. So, since the signal bin index is known (as $f_0 \equiv f_L$ is known for pilot symbols), the reasonable flat fading characterizing the propagation and the properties of DFT allow the channel to be reliably estimated as a complex gain $\tilde{h} = Y_{\mathrm{DC}}[0]/2^{\mathrm{SF}}$ measured with respect to the 0-th bin of Y_{DC} (the symbol transmit power is normalized to 1 as in eq. (2)). In general, the reliability of $\tilde{h}$ is proportional to the SNR since it depends on the level of noise with respect to the received signal power (the inaccuracy of estimation may be also due to imperfect synchronization causing the signal components shift in $Y_{\mathrm{DC}}[k]$).

Regarding detection, the symbol-by-symbol demodulation can be performed according to eq. (5) applied to the portion of $y[n]^{(s)}$ where the packet is present and according to the estimated time of arrival $\tilde{\Delta}_s$. To this aim, it is worth noting that the s-th packet to be decoded may be corrupted by interfering components due to the overlap of other packets still to be processed. Such occurrence results in the example described in Fig. 3(c), so it follows that signal detection may be subject to errors. However, the synchronization achieved according to eqs. (9)-(10) guarantees that the s-th packet currently under processing is that one received with the highest power among many others potentially overlapping in $y^{(s)}[n]$. In such scenario, the dechirping-based demodulation results as reliable even in the presence of interference. In fact, eq. (5) returns the decision on the symbol as taken basing on the highest frequency component characterizing the received signal, that reasonably belongs to the s-th packet. The other smaller frequency components are instead not considered, since referring to weaker packets. Finally, decoding errors may potentially occur anyway. In this regard, in the next section we show how the GW diversity can be conveniently exploited to further improve the packet detection.

C. Recursive SIC

As previously outlined, synchronization and decoding are performed considering the packets in descending order of power, and not in order of arrival. In this direction, the signal component of the s-th packet just decoded can be finally removed from $y^{(s)}[n]$, making the decoding of the other weaker packets be possible. Specifically, by decoding the s-th packet, the GW identifies the index of the LoRa symbols gathered in the payload $q_s[n]$, decided according to eq. (5). It follows that, given the knowledge of LoRa signaling waveform, the GW is able to compute the signal shape referring to the decoded packet. We recall that the preamble is known by the GW and following instead eq. (5) we can obtain a *decided* version of the the payload $\hat{q}_s[n]$ given by the sequence of decided LoRa symbols, generically referred as $\hat{x}_i$ ($i \in \{0, 1, ..., 2^{\mathrm{SF}}\text{-}1\}$). Finally, by exploiting the information about the s-th LoRa packet previously processed, that is the time of arrival $\tilde{\Delta}_s$ and the channel estimate $\tilde{h}_s[n]$, we can implement the SIC mechanism as:

$$y^{(s+1)}[n] = y^{(s)}[n + \tilde{\Delta}_s] - (\hat{p}_s[n - \tilde{\Delta}_s] * \tilde{h}_s[n]) \qquad (12)$$

where $\hat{p}_s[n]$ (with n = 0,1,...,L_p-1) is removed from the overall signal window $y^{(s)}[n]$. From eq. (12), $y^{(s+1)}[n]$ represents the signal of the GW where the strongest packet has been removed from, so that it can be considered in the next $(s+1)$-th algorithm iteration for the search for other packets. The use of SIC allows the highest peak in $R^{(s)}_{yz}[n]$ to be removed so that, when performing the synchronization on $y^{(s+1)}[n]$, the second strongest signal in $y^{(s+1)}[n]$ is detectable (Fig. 5(b)). So, the procedure continues until eq. (9) reveals the presence of (possibly) all the packets (Fig. 5(c)). Summarizing, the proposed algorithm for interference cancellation (to be performed at the single GW) allows overlapping LoRa packets to be synchronized and decoded in a sequential fashion. Such solution is very effective to resolve the capture effect. In fact, by means of SIC, the GW decodes the strongest packet and then subtracts it from the overall signal in the receiving time window, so that the shadowing effect caused by the strongest signal is removed and the remaining weakest packets can be detected as well. Of course, the larger the packets time difference of arrival is, the more reliable the synchronization based on eq. (9) is. Furthermore, it can be observed from eq. (12) that the accuracy of cancellation relies on the reliability of channel estimation and payload decoding that, in turn, depend on the signals SNR and on the colliding packets power difference.

IV. Combined decoding based on gateway diversity: BiDiCom

Since LoRa communication is essentially broadcast, the packet transmitted by the u-th ED could be received by multiple GWs that forward the decoded data to the NS (for the sake of completeness, note that each GW is also responsible for error control, however deepening this aspect goes beyond the scope of this work). Finally, the NS performs the packets deduplication on the basis of additional information received by the GWs about the packet SNR and RSSI. So, if a further integrity check is passed, the information is forwarded to the application servers, otherwise the procedure for packet retransmission request is activated. The current LoRaWAN implementation entails all the packets arriving at the NS to be as collision free, thus meaning that synchronization and data decoding at the GW side are performed in absence of interference. On the other hand, the proposed SIC-based

algorithm allows LoRa packets to be potentially decoded even in presence of interference. In that case, since the reliability of decoding depends not only on the channel effect but also on the interference level, it follows that parameters like SNR and RSSI are not enough to measure the quality of the message received by the NS, and deduplication may be no more the most effective way for information selection.

Before we proceed, two important aspects must be underlined. Firstly, although the reliability of a link with high SNR is in general higher than the reliability of a link with low SNR, it is not assured that the presence of an error in the best link implies necessarily the same error as occurring in the worst link as well. For example, let us consider the transmission of a 10 bits sequence composed of all 0s. Due to the channel effect, the signal detection over the best link returns an error on the last bit of the sequence, decided as a 1. Moving to the signal detection on the worst link, it is reasonable to expect even multiple errors. However, it is not proved that an error must necessarily occur on the last bit. In fact, for instance we may have the first five bits wrongly decoded, while the last five ones are correct. From this example it can be inferred that different copies of the same received information can be conveniently combined to achieve a more reliable detection. The second issue to consider regards the impact of interference and channel quality. It may happen that the communication over a good channel but subject to strong interference is less reliable than the communication occurring on a bad channel but with low interference. In this direction, it is interesting to note that the EDs position and the different propagation delays make the measured LoRa packets mutual interference varying from GW to GW. So, we propose a novel mechanism to be implemented at the NS that realizes a weighted combining of multiple copies of the same packet received by different GWs, in order to achieve a more reliable data decoding. Such technique is referred as Bit Diversity Combining (BiDiCom) since exploiting GW diversity to realize information combining at bit level.

A. BiDiCom implementation

Let us consider the LoRa packet transmitted by the u-th ED and received by G GWs. The packet payload is supposed to carry L_b bits. After synchronization and decoding performed following the algorithm in Sec. III, the g-th GW ($g = 1, 2, ..., G$) forwards to the NS the information bits extracted from the packet payload, described by the sequence $M_{g,u} = \{b_1^{(g,u)}, b_2^{(g,u)}, ..., b_\ell^{(g,u)}, ..., b_{L_b}^{(g,u)}\}$. Following an antipodal binary representation, the ℓ-th element of the sequence (ℓ=1,2,...,L_b) is given as $b_\ell^{(g,u)} = \pm 1$. The links between GWs and NS are meant to be reliable, so $M_{g,u}$ is reasonably assumed as received without errors. The exploitation of GW diversity allows the NS to collect G bit sequences referring to the same packet that are, in general, different. The proposed BiDiCom operates a weighted sum of the available G sequences, defined as $M_{C,u} = \sum_{g=1}^{G} w_{g,u} M_{g,u}$, where $w_{g,u}$ is the weighting coefficient associated to the information received by the g-th GW. As the combining is realized at bit level, we have:

$$b_\ell^{(C,u)} = \sum_{g=1}^{G} w_{g,u} b_\ell^{(g,u)} =$$

$$= w_{1,u} b_\ell^{(1,u)} + w_{2,u} b_\ell^{(2,u)} + ... + w_{g,u} b_\ell^{(g,u)} + ... + w_{G,u} b_\ell^{(G,u)} \tag{13}$$

representing the ℓ-th binary element of $M_{C,u}$, resulting from combining. The weighting coefficient $w_{g,u}$ is related to reliability of the u-th packet decoded by the g-th GW. So it represents a combined measure of two independent aspects, that are the link quality and the interference characterizing the packet transmission from the u-th ED to the g-th GW. The first one is related to the channel conditions between the u-th ED and the g-th GW. In this regard, basing on the channel estimate information retrieved as in Sec. III-B, we have that the reliability of $M_{g,u}$ can be measured according to the following coefficient:

$$w_{g,\mathrm{H}} = \frac{|\tilde{h}_{g,u}|^2}{\sum_{j=1}^{G} |\tilde{h}_{j,u}|^2} \tag{14}$$

that is essentially the cost function characterizing the normalized Maximal Ratio Combining technique [27], returning real valued weighting coefficients so that $0 \leq w_{g,\mathrm{H}} \leq 1$, where the subscript $(\cdot)_\mathrm{H}$ is related to the channel. The second aspect to be to be taken into account when measuring the reliability of the g-th copy of the u-th packet is the level of interference caused by other superposing LoRa signals, expressed by the coefficient $w_{g,\mathrm{I}}$, with the subscript $(\cdot)_\mathrm{I}$ being related to the interference. In order to define $w_{g,\mathrm{I}}$, let us consider eq. (6) and the reference example in Fig. 3(c), where it is shown how demodulation based on eqs. (4)-(5) is prone to errors if there are multiple peaks in $|Y_{\mathrm{DC}}[k]|$ very close in amplitude. In this direction, the evaluation of the decoding reliability can be extended from the single LoRa symbol to the entire packet case. Specifically, given U overlapping packets, the decoding of the u-th one suffers from the interference caused by the other D=U-1 signals. In principle, the SIC algorithm in Sec. III returns as available the estimates $\tilde{h}_{g,u}$ referring to the channel between the u-th ED and the g-th GW and $\tilde{h}_{g,d}$ describing the link between the d-th ED, acting as interference for the u-th ED (d=1,2,...,D), and the g-th GW. Moreover, the packets time of arrival are also estimated at the g-th GW, referred as $\tilde{\Delta}_{g,u}$ for the u-th packet and $\tilde{\Delta}_{g,d}$ for the d-th packet, respectively. So, we can calculate the desynchronization $\phi_{g,u,d} = |\tilde{\Delta}_{g,u} - \tilde{\Delta}_{g,d}|$ between the signals coming from the u-th and d-th user, employed to define the term γ_g as:

$$\gamma_g = \min_{d=1,2,...,D, d \neq u} \frac{|\tilde{h}_{g,u} - \tilde{h}_{g,d} \Delta\phi_{g,u,d}|}{\tau_w} \tag{15}$$

that essentially weights the power difference between the u-th packet under processing and the interfering signal with closest power. The term τ_w represents a normalization factor set according to the receiver sensitivity. Finally, the weighting coefficient related to the effect of interference on the link

between the u-th ED and the g-th GW is defined as:

$$w_{g,\mathrm{I}} = \begin{cases} \dfrac{\gamma_g}{\gamma_g + 1}, & D > 0 \\ 1, & D = 0 \end{cases} \tag{16}$$

with values approaching 1 as γ_g grows (that is, for low levels of interference). As previously outlined, channel quality and interference refer to independent aspects, so even $w_{g,\mathrm{H}}$ and $w_{g,\mathrm{I}}$ are considered as separated. Therefore, in general, $w_{g,u}$ is given as:

$$w_{g,u} = w_{g,\mathrm{H}} \cdot w_{g,\mathrm{I}} \tag{17}$$

that is the product of $w_{g,\mathrm{H}}$ and $w_{g,\mathrm{I}}$, returning real and positive valued coefficients. By doing so, eq. (13) results in a soft bit combining since the ℓ-th element $b_\ell^{(C,u)}$ is in general real as well. Furthermore, in the particular case where the u-th packet is interference free (U=1, hence D=0), $w_{g,\mathrm{I}}$ is equal to 1 so that eq. (17) becomes function of only $w_{g,\mathrm{H}}$. As the last step, a hard decision mechanism is implemented to return $b_\ell^{(C,u)}$ as a binary element equal to $+1$ when $b_\ell^{(C,u)} \geq 0$ or equal to -1 if $b_\ell^{(C,u)} < 0$. So $M_{C,u}$ is the result of decoding performed with BiDiCom, the reliability of which is tied to the convenient combining of the information coming from different copies of the same LoRa packet.

B. On the feasibility of combining in LoRaWAN

The proposed BiDiCom is aimed to make the best of GW diversity by considering that LoRaWAN does not provide inter-GW communication and so signal combining cannot be implemented. In order to overcome such problem, the solution we present is instead oriented to *bit combining*. By doing so, processing concerns the information stream retrieved from the packets by the GWs and forwarded to the NS, hence allowing the network traffic to remain fundamentally unaltered. BiDiCom realizes bit combining according to the mechanism in eq. (13), that provides backward compatibility with deduplication as well. In fact, by simply setting equal to 1 the combining coefficient (eq. (17)) related to the packet copy to be saved and to 0 all the remaining ones, it is possible to realize the standard deduplication.

Concerning signal processing effort and delay, both the proposed BiDiCom and SIC require the simple computation of sums and products that, however, may introduce some uplink and downlink latency. In this regard, in LoRaWAN-based IoT applications, the quality-of-service constraints concern coverage and low power consumption. Therefore, latency is not a problem for uplink. On the other hand, for those LoRaWAN networks relying on confirmed-data packets, latency may impact on feedback signaling performance since, if the ED does not receive the feedback within specific time windows, it proceeds with packet retransmission even if not necessary. Such issue may be problematic especially for class A devices, that use two short receiving time windows to detect the potential packet acknowledgment. Hence, given U_i interfering packets, the SIC and BiDiCom processing delay impacting on downlink is tolerable until the packet round trip time, namely RTT_{U_i}, is shorter than the time occurring between the end of ED packet transmission and the start of the second receiving time window, referred as Δ_2. In this direction, we must have that:

$$\mathrm{RTT}_{U_i} = T_{\text{uplink}} + T_{\text{downlink}} =$$

$$T_{e,\mathrm{PKT}} + T_{p,\mathrm{GW}} + (U_i \cdot T_{\mathrm{SIC,GW}}) + T_{\mathrm{BiDiCom,NS}} + T_{e,\mathrm{ACK}} \leq \Delta_2 \tag{18}$$

where $T_{e,\mathrm{PKT}}$ is the packet time on air, $T_{p,\mathrm{GW}}$ is the time required for detecting a single, incoming signal at the GW, $T_{\mathrm{SIC,GW}}$ is the processing time required for the single iteration of the SIC, $T_{\mathrm{BiDiCom,NS}}$ is the time required for computing BiDiCom and $T_{e,\mathrm{FB}}$ is the time on air of the (potentially) emitted feedback. In eq. (18), we do not consider the signals propagation delay since it can be reliably assumed as negligible with respect to the packet time on air. Furthermore, in downlink, the GW acts simply as relay, so the corresponding processing has been neglected as well. It is worth highlighting that SIC processing delay suffered from a packet at GW side is proportional to which SIC iteration is considered for its detection. From eq. (18), the term $T_{p,\mathrm{GW}} + (U_i \cdot T_{\mathrm{SIC,GW}})$ essentially refers to the worst case where the packet of interest is detected at the very last SIC iteration (that is, other N_i packets are detected first).

Overall, BiDiCom supported and SIC-based mechanism essentially address such issues at the physical layer, thus allowing the current lightweight LoRaWAN implementation to be unaltered, especially regarding the ALOHA like channel access. So, even the network nodes functionalities do not need any upgrade or modification. Finally, it is worth noting that LoRa communications may suffer not only from intrinsic interference, but also from inter-technology interference caused by other signaling coming from different services [28]. Interestingly, the exploitation of gateway diversity provides more robustness even to such external impairments.

V. Numerical results

In this section, we discuss the performance of both the proposed techniques by analyzing the results of some simulations performed in Matlab. Specifically, we first evaluate the reliability of the SIC-based algorithm implemented at the GW, then we consider a LoRa/LoRaWAN network scenario where to measure the performance of BiDiCom mechanism.

A. Interference mitigation performance

In order to investigate the effectiveness of the proposed scheme for interference mitigation, we consider the presence of 3 overlapping LoRa packets, transmitted with the same power, same SF, and received by a single reference GW. The packet length is 50 bytes and assumed to be known by the GW. The transmitting EDs are supposed to work over the same bandwidth and using the same SF, so that interference occurs. The packets time of arrival is randomly sorted in time, so to simulate different cases of signal overlap. The power of the packets P_u (u=1,2,3) is instead sorted by decreasing order, so that P_1 and P_3 refer to the strongest and weakest signal, respectively. Furthermore, we define $\mathrm{PR} = 10\log_{10}\frac{P_\alpha}{P_\beta}$ ($\alpha = 2, 3, \beta = \alpha$-1, $\alpha \neq \beta$) as the power ratio between

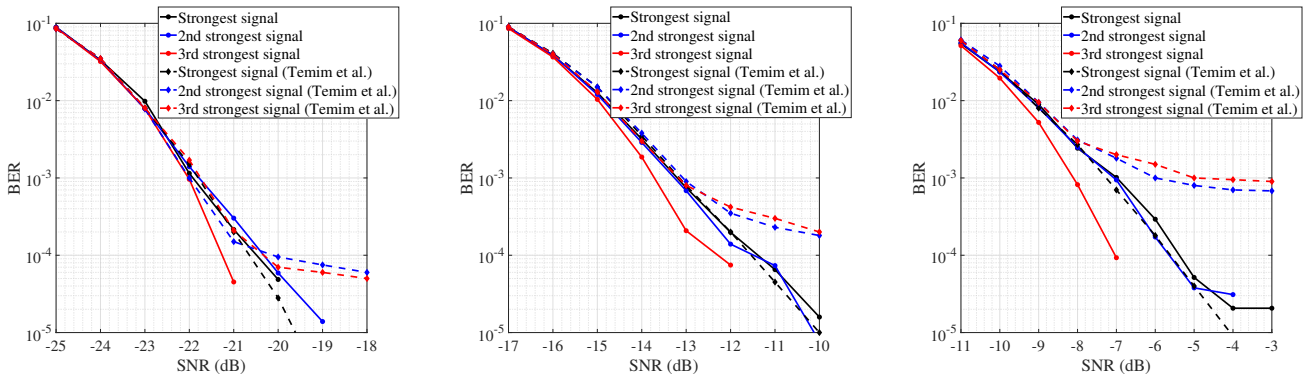

(a) SF=12, PR=6 dB (b) SF=9, PR=6 dB (c) SF=7, PR=6 dB

Fig. 6. BER performance as a function of SF and PR.

P_1 and P_2, and P_2 and P_3. The higher PR is, the lower the effect of packet mutual interference on signal detection is. In such simulation framework, we were able to provide a performance comparison between the proposed technique and the interference cancellation method presented by *Temim et al.* in [17]. Differently from our method, in [17] packet decoding and SIC are performed by exploiting the estimation of the signals time offset. Specifically, performance are shown in terms of bit error rate (BER), measured for each of the 3 received packets as a function of the SNR. Simulation results have been averaged on 10^4 runs. Fig. 6 shows the curves for 3 different configurations, that is considering SF=12 and PR=6 dB, SF=9 and PR=6 dB, SF=7 and PR=6 dB. Solid curves refer to the proposed mechanism, while dotted curves refer to the method in [17]. From Fig. 6(a) it is possible to observe that the two considered solutions provide essentially the same performance, with BER approaching 10^{-5} as the SNR increases. In that case, the effectiveness of cancellation is mainly due to the properties of LoRa signaling. In fact, having SF=12 allows the signals to be long in time and more robust to decoding failure. On the other hand, when the SF is reduced, frame synchronization and decoding become more challenging. In this regard, by referring to Figs. 6(b)-6(c), we can appreciate that the proposed method outperforms that one presented in [17]. In detail, some interesting aspects must be highlighted. First, for increasing values of SNR, the BER measured on the intermediate and weakest power signals becomes flat when applying the mechanism in [17]. Differently, the curves measured with the proposed interference cancellation method maintain a linear like behavior (on a logarithmic scale), thus reflecting in the achievement of a lower BER. Furthermore, it can be noted that, with the mechanism in [17], the highest reliability is achieved for the packet received with the strongest power, while on the other hand the proposed method returns the weakest signal decoding as the most efficient one. Such result can be explained by recalling the nature of the interference cancellation algorithm in Sec. III, that allows the synchronization and decoding of LoRa packets following not the order of arrival, but the descending order of signals power. So, having the weakest signal as the last one processed means that it is ideally decoded in absence of interference, since the other stronger signals have been canceled during the previous algorithm iterations. The achievement of good performance in terms of BER reveals that packet synchronization and interference cancellation are performed efficiently. In fact, we measured an average packet misdetection percentage equal to the 0.03%, thus meaning that synchronization is almost always achieved.

B. BiDiCom performance

The second part of the analysis concerns the performance of the proposed BiDiCom mechanism relying on gateway diversity. The simulation framework considers the presence of 10000 EDs randomly deployed in a squared urban area of 16 km^2. The EDs are supposed to be active in the band EU863, defining the range 863-870 MHz, with transmit power set to 14 dBm by LoRa specifications. Since simulations do not deal with feedback signaling analysis, whatever type of class can be assumed for devices. The EDs packet traffic is generated following a Poisson model, ruled by the parameter λ ranging from 1 to 6 pkt/hour. The EDs are assumed to transmit on the same 125 kHz bandwidth slot and using the same SF, so that interference occurs from overlapping communications. The packet payload is set to 50 bytes, and the coding rate is CR=4/5. Specifically, SFs=7,8,9 were considered for simulations. The goal is to evaluate the effectiveness of BiDiCom with respect to decoding achieved by applying the conventional packet deduplication at the NS. The performance are expressed in terms of BER, measured as a function of the position of the transmitting ED with respect to GWs. So, the results are presented in form of map, where each point corresponds to a squared area of width 50 meters where the ED is supposed to be deployed. The sum of packets transmitted for each ED position corresponds to 10^6 bits. Furthermore, BER has been averaged on 10 simulations in order to achieve more accurate results. In general, performance are expected to be strictly dependent of the number and position of GWs within the considered area, with the ideal scenario being characterized by the GWs as uniformly distributed in space. Differently, we refer to one real environment related to Dortmund (51°29'51"N, 7°28'08"E) wit 8 GWs as reported in the ThingsNetwork platform map at the end of 2020

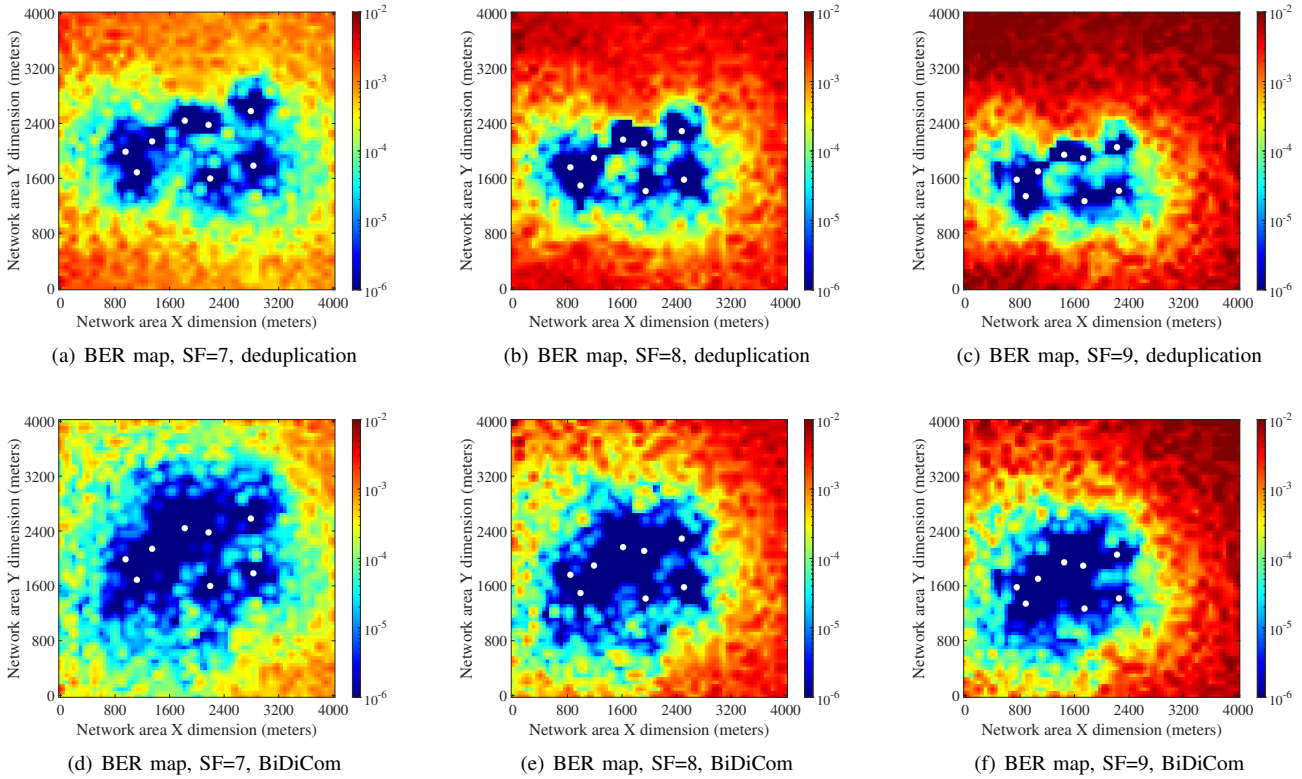

(a) BER map, SF=7, deduplication (b) BER map, SF=8, deduplication (c) BER map, SF=9, deduplication

(d) BER map, SF=7, BiDiCom (e) BER map, SF=8, BiDiCom (f) BER map, SF=9, BiDiCom

Fig. 7. BER performance in Dortmund scenario with GW=8, considering SF=7,8,9.

[29]. Furthermore, we consider each GW as implementing the proposed SIC scheme introduced in Sec. III, so allowing both packet deduplication and BiDiCom to work even in the presence interference. Figs. 7 report the BER maps obtained considering deduplication and BiDiCom. The GWs position is represented by white circled points. Figs. 7(a-d) show the performance when SF=7. Specifically, BER around 10^{-6} is achieved when the ED is very close to any of the available GWs, since the high power of the received packet is dominant with respect to the interfering signals. On the other hand, performance decrease for longer links where the impact of other concurrent signals becomes more relevant. Interestingly, it is possible to appreciate how BiDiCom outperforms conventional deduplication. In fact, the blue and green areas in Fig. 7(d) measuring low BER are significantly widened with respect to what observed in Fig. 7(a). Such result is also evident in Figs. 7(b-e) and Figs. 7(c-f) where SF=8 and SF=9 is considered, respectively. Furthermore, it can be noted that the BER measured for EDs placed far from the GWs increases as the SF grows. At first glance, such result is in contrast with the expected LoRa performance, since the increase of the SF makes the received signal more robust and, therefore, the detection more reliable. Actually, it is fundamental to highlight that the use of a high SF provides better performance only when referring to an interference free scenario, that is the condition where there is no packet collision. Differently, our analysis is focused on the detection and decoding of overlapping packets, made possible thanks to the implementation of the proposed SIC-base algorithm. According to the characteristics of LoRa modulation, the use of high order SFs allows the signal to be longer in time, so that detection at the GW side results more robust to the channel effects. However, by doing so, the EDs channel occupation time increases, and the probability of experiencing interference of other packets grows as well, making the communication more prone to errors. In this regard, the use of BiDiCom counterbalances the unreliability of decoding due to interference and allows the use of a small SF even for large communication ranges. Such result is confirmed by the curves in Fig. 8(a), showing the BER performance as a function of the number of GWs involved in BiDiCom (despite the presence of 8 GWs, it is not assured that a packet is always correctly detected by all). In fact, it can be seen that using SF=7 allows the achievement of the lowest BER, and performance improve as the number of available GWs for BiDiCom grows. Moreover, in Fig. 8(b) we show the average BER performance as a function of the number of EDs simultaneously connected to the network. Specifically, the presence of an increasing number of EDs leads the collision probability to grow as well, hence BER lowers. However, BiDiCom always outperforms deduplication, providing best results when a low SF is used.

Finally, we pass to detail the LoRaWAN network performance in terms of latency, in order to verify the feasibility of SIC and BiDiCom processing. By assuming the transmission of a 50 byte payload packet from a class A ED, we calculated the corresponding RTT_{U_i} for different SF scenarios. Tab. II shows the resulting values of RTT_{U_i}, expressed in milliseconds, and the parameters used for its computing according to

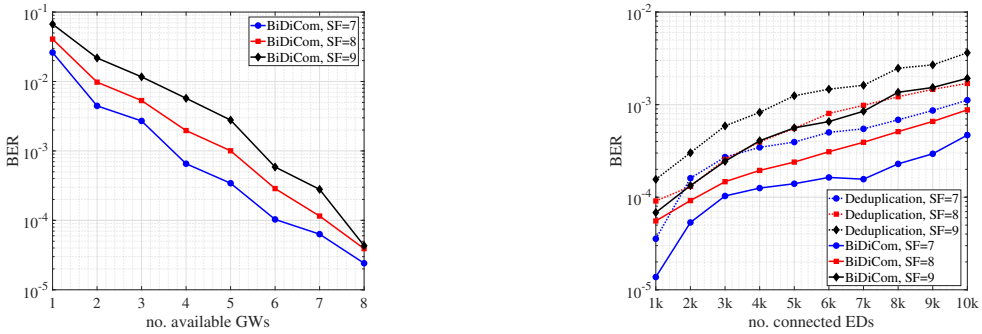

(a) (b)

Fig. 8. BER performance as a function of the number of GWs involved in BiDiCom (a) and the number of connected EDs (b).

TABLE II
MEASURED LORAWAN NETWORK LATENCIES AND PACKET RTT

SF	U_i	$T_{e,\text{PKT}}$(ms)	$T_{p,\text{GW}}$(ms)	$T_{\text{SIC,GW}}$(ms)	$T_{\text{BiDiCom,NS}}$(ms)	$T_{e,\text{ACK}}$(ms)	RTT_{U_i}(ms)
7	1.82	97.2	67.6	17.3	0.4	41.2	237.8
8	3.29	174.7	218.1	35.2	0.5	72.2	581.3
9	5.81	308.5	378.6	48.1	0.6	144.4	1111.6

TABLE III
PACKET ERROR RATE (PER) RESULTS

Scenario	**Conventional GW decoding and Deduplication**	**SIC-based GW decoding and Deduplication**	**SIC-based GW decoding and BiDiCom**
SF=7, GW=8	0.294	0.047	0.025
SF=8, GW=8	0.420	0.064	0.025
SF=9, GW=8	0.589	0.109	0.074

in eq. (18). In detail, U_i represents the average number of interfering packets measured during network simulations, $T_{e,\text{PKT}}$ and $T_{e,\text{ACK}}$ are directly taken or derived according to table 6 in [30]. The processing times $T_{p,\text{GW}}$, $T_{\text{SIC,GW}}$, $T_{\text{BiDiCom,NS}}$ have been measured during Matlab simulations operations. The computation was performed exploiting a 2.5 GHz single core CPU that is actually more powerful than current GWs hardware, hence the values in Tab. II were rescaled so as to match with the capability of a 1.3 GHz single core processor typically equipping commercial GWs. However, we highlight that Matlab software runs over an operating system that performs other operations in background, so the processing times measured during simulations are overdimensioned. Since class A devices consider a delay Δ_2=2 seconds between the end of packet transmission and the beginning of the last receiving time window, we can appreciate from Tab. II that the RTT is far below Δ_2, so no problems of latency occur. Of course, by increasing the SF up to 12, the RTT is expected to grow, but this is mainly due to increase of packet time on air that has a higher impact on RTT than processing delays. However, we recall that with BiDiCom it is preferable to use low SF. So, even from this point of view, the proposed solution results perfectly tailored to LoRaWAN.

C. Packet error rate and ED power consumption

By neglecting the effect of coding and assuming that a packet is correctly received only if error free, we define the packet error rate (PER) as the ratio between the packets decoded with at least on error bit and the total number of transmitted packets. For the network scenario considered in Sec. V-B, we measure the average PER for different SF, with results reported in Tab. III. Specifically, PER is calculated for three LoRaWAN architectures, considering conventional decoding at GW side and deduplication at the NS (that is, the current LoRaWAN implementation), SIC based decoding at the GW and deduplication at the NS, SIC based decoding at the GW and BiDiCom at the NS, respectively. From Tab. III, it can be appreciated how the current implementation of LoRaWAN (left column) is totally inefficient in dense network scenarios with high probability of interference among signals. On the other hand, with SIC it is possible to decode colliding packets, thus allowing a significant reduction of PER. Moreover, the use of BiDiCom in place of deduplication provides a further improvement in terms of packet decoding reliability.

The measure of PER allows to take into account the number of retransmitted packets for computing the total number of packets sent by the ED. Given N_t as the number of daily packets to be transmitted from the ED, we have that the number of packets actually transmitted, taking into account the potential retransmissions, is $N_{tot} = \sum_{m=0}^{M} N_t(\text{PER})^m$, with M being the highest integer number so that $\lfloor N_t(\text{PER})^m \rfloor < 1$. The number of transmitted packets N_{tot} can be used to estimate the ED power consumption. In this regard, we refer to

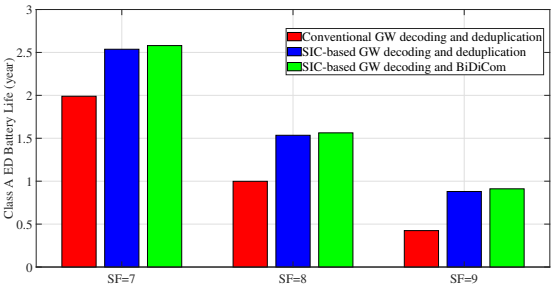

Fig. 9. Battery life for class A ED as a function of SF and LoRaWAN implementation.

class A ED, for which Semtech Corporation has provided some documentation [31], [32]. In detail, the daily battery capacity C_{TOT} consumed by a class A ED, measured in milliampere, is function of the energy spent in active and idle mode, namely C_{ON} and C_{OFF}, that is:

$$C_{\text{TOT}} = C_{\text{ON}} + C_{\text{OFF}} =$$

$$= \left(\frac{N_{tot}}{T}(I_{tx}\cdot t_{tx} + I_{rx}\cdot t_{rx})\right) + \left(I_s(24 - (t_{tx}+t_{rx})\frac{N_{tot}}{T})\right) \quad (19)$$

where I_{tx}, I_{rx} and I_s are the current level when the ED is in transmit, receive and idle mode, respectively, t_{tx} and t_{rx} is the time spent by the device in transmit and receive mode, respectively, and T is the number of milliseconds per hours. Given C_{ED} as the device battery capacity, measured in milliampere-hour, we have that:

$$BL = \frac{C_{\text{ED}}/C_{\text{TOT}}}{24 \cdot 364,25} \quad (20)$$

expresses in years the battery life for a class A ED. Following eqs. (19)-(20), we calculate the battery life for a class A ED for the three cases of LoRaWAN architectures described in Tab. III, regarding the Dortmund network scenario where 8 GWs are available. Specifically, we consider and ED as generating 4 pkt/hour, that is 96 pkt/day, with payload equal to 50 bytes and time on air (that corresponds to t_{tx} in eq. (19)) depending on the SF. The device battery capacity is chosen as equal to C_{ED}=2500 mAh, that represents a low-medium value for IoT sensors. The results are shown in Fig. 9, where it is possible to appreciate how the use of SIC and BiDiCom provides a significant energy saving due to the capability of decoding colliding packets and thus reducing the retransmissions. Of course, the increase of the SF causes a larger power consumption since the ED spends more time in transmit mode. However, this aspect does not depend on the mechanism used for packet detection.

VI. Conclusion

In this contribution, we first presented an algorithm for interference mitigation among LoRa signals overlapping at the GW, which reduces the necessity of packet retransmission in LoRaWAN as well. Furthermore, we proposed a bit combining mechanism that exploits the gateway diversity to achieve a more reliable packet decoding. The results have shown that the joint use of the proposed techniques allows the reliability of LoRa communication to be improved for any considered SF. Therefore, the use of low SFs is shown to be feasible even for a wide communication range. As a consequence, the activity time of EDs is reduced, with energy consumption being limited as well.

References

[1] U. Raza, P. Kulkarni, and M. Sooriyabandara, "Low power wide area networks: An overview," *IEEE Communications Surveys & Tutorials*, vol. 19, no. 2, pp. 855–873, 2017.

[2] Semtech Corporation, "What is LoRa?" *https://www.semtech.com/lora/what-is-lora*, 2020.

[3] LoRa Alliance, "LoRaWAN Specifications," *https://lora-alliance.org/resource-hub/lorawanr-specification-v11*, 2020.

[4] J. F. Kurose and K. Ross, *Computer networking: A top-down approach featuring the Internet*, 6th ed. Addison-Wesley, 2001.

[5] J. P. Shanmuga Sundaram, W. Du, and Z. Zhao, "A survey on LoRa networking: Research problems, current solutions, and open issues," *IEEE Communications Surveys Tutorials*, vol. 22, no. 1, pp. 371–388, 2020.

[6] J. Lim and Y. Han, "Spreading factor allocation for massive connectivity in LoRa systems," *IEEE Communications Letters*, vol. 22, no. 4, pp. 800–803, 2018.

[7] F. Cuomo, M. Campo, A. Caponi, G. Bianchi, G. Rossini, and P. Pisani, "EXPLoRa: Extending the performance of LoRa by suitable spreading factor allocations," in *2017 IEEE 13th International Conference on Wireless and Mobile Computing, Networking and Communications (WiMob)*, 2017, pp. 1–8.

[8] L. Beltramelli, A. Mahmood, P. Osterberg, and M. Gidlund, "LoRa beyond ALOHA: An investigation of alternative random access protocols," *IEEE Transactions on Industrial Informatics*, pp. 1–1, 2020.

[9] J. Ortin, M. Cesana, and A. Redondi, "Augmenting LoRaWAN performance with listen before talk," *IEEE Transactions on Wireless Communications*, vol. 18, no. 6, pp. 3113–3128, 2019.

[10] B. Reynders, Q. Wang, P. Tuset-Peiro, X. Vilajosana, and S. Pollin, "Improving reliability and scalability of LoRaWANs through lightweight scheduling," *IEEE Internet of Things Journal*, vol. 5, no. 3, pp. 1830–1842, 2018.

[11] W. Wu, Y. Li, Y. Zhang, B. Wang, and W. Wang, "Distributed queueing-based random access protocol for LoRa networks," *IEEE Internet of Things Journal*, vol. 7, no. 1, pp. 763–772, 2020.

[12] N. E. Rachkidy, A. Guitton, and M. Kaneko, "Decoding superposed LoRa signals," in *2018 IEEE 43rd Conference on Local Computer Networks (LCN)*, 2018, pp. 184–190.

[13] L. Vangelista and A. Cattapan, "Start of packet detection and synchronization for LoraWAN modulated signals," *IEEE Transactions on Wireless Communications*, pp. 1–1, 2021.

[14] U. Noreen, L. Clavier, and A. Bounceur, "LoRa-like CSS-based PHY layer, capture effect and serial interference cancellation," in *European Wireless 2018; 24th European Wireless Conference*, 2018, pp. 1–6.

[15] R. Eletreby, D. Zhang, S. Kumar, and O. Yagan, "Empowering low-power wide area networks in urban settings," *Proceedings of the Conference of the ACM Special Interest Group on Data Communication (SIGCOMM '17)*, pp. 309–321, 2017.

[16] X. Xia, Y. Zheng, and T. Gu, "FTrack: Parallel decoding for LoRa transmissions," *IEEE/ACM Transactions on Networking*, vol. 28, no. 6, pp. 2573–2586, 2020.

[17] M. A. Ben Temim, G. Ferre, B. Laporte-Fauret, D. Dallet, B. Minger, and L. Fuche, "An enhanced receiver to decode superposed LoRa-like signals," *IEEE Internet of Things Journal*, vol. 7, no. 8, pp. 7419–7431, 2020.

[18] A. Dongare, R. Narayanan, A. Gadre, A. Luong, A. Balanuta, S. Kumar, B. Iannucci, and A. Rowe, "Charm: Exploiting geographical diversity through coherent combining in low-power wide-area networks," in *2018 17th ACM/IEEE International Conference on Information Processing in Sensor Networks (IPSN)*, 2018, pp. 60–71.

[19] LoRa Alliance, "LoRaWAN regional parameters," *https://lora-alliance.org/sites/default/files/2018-04/lorawantm_regional_parameters_v1.1rb_-_final.pdf*, 2017.

[20] E. Aras, G. S. Ramachandran, P. Lawrence, and D. Hughes, "Exploring the security vulnerabilities of LoRa," in *2017 3rd IEEE International Conference on Cybernetics (CYBCONF)*, 2017, pp. 1–6.

This article has been accepted for publication in a future issue of this journal, but has not been fully edited. Content may change prior to final publication. Citation information: DOI 10.1109/TWC.2022.3172629, IEEE Transactions on Wireless Communications

[21] D. Bankov, E. Khorov, and A. Lyakhov, "On the limits of LoRaWAN channel access," in *2016 International Conference on Engineering and Telecommunication (EnT)*, 2016, pp. 10–14.
[22] D. Croce, M. Gucciardo, S. Mangione, G. Santaromita, and I. Tinnirello, "Impact of LoRa imperfect orthogonality: Analysis of link-level performance," *IEEE Communications Letters*, vol. 22, no. 4, pp. 796–799, 2018.
[23] L. Vangelista, "Frequency shift chirp modulation: The LoRa modulation," *IEEE Signal Processing Letters*, vol. 24, no. 12, pp. 1818–1821, 2017.
[24] R. El Chall, S. Lahoud, and M. El Helou, "LoRaWAN network: Radio propagation models and performance evaluation in various environments in Lebanon," *IEEE Internet of Things Journal*, vol. 6, no. 2, pp. 2366–2378, 2019.
[25] M. Hata, "Empirical formula for propagation loss in land mobile radio services," *IEEE Transactions on Vehicular Technology*, vol. 29, no. 3, pp. 317–325, 1980.
[26] O. Afisiadis, M. Cotting, A. Burg, and A. Balatsoukas-Stimming, "On the error rate of the LoRa modulation with interference," *IEEE Transactions on Wireless Communications*, vol. 19, no. 2, pp. 1292–1304, 2020.
[27] J. G. Proakis and M. Salehi, *Digital Communications*, 5th ed. McGraw-Hill, 2008, Chapter 13.
[28] J. Haxhibeqiri, A. Shahid, M. Saelens, J. Bauwens, B. Jooris, E. De Poorter, and J. Hoebeke, "Sub-gigahertz inter-technology interference. how harmful is it for LoRa?" in *2018 IEEE International Smart Cities Conference (ISC2)*, 2018, pp. 1–7.
[29] The Things Network, *https://www.thethingsnetwork.org/map*.
[30] L. Casals, B. Mir, R. Vidal, and C. Gomez, "Modeling the energy performance of LoRaWAN," *Sensors*, vol. 17, no. 10, 2017.
[31] Semtech Corporation, "An in-depth look at LoRaWAN class A devices," *https://lora-developers.semtech.com*, 2019.
[32] ——, "Class A devices battery life and capacity," *https://lora-developers.semtech.com/documentation/tech-papers-and-guides*, 2022.

Andrea Petroni received the B.Sc., M.Sc. degrees in electronics engineering in 2011 and 2014, respectively, and the Ph.D. degree in Information and Communication Technology in 2018 from the Sapienza University of Rome, Rome, Italy. He is currently a Postdoctoral Research Fellow with the Department of Information, Electronics, and Telecommunication Engineering, Sapienza University of Rome. His general research interests include wireless digital communications and signal processing, with applications to underwater acoustic communications and optical communications. He is also working on Low Power Wide Area Networks for healthcare monitoring and LoRa technology for IoT applications.

Mauro Biagi (S'99-M'05-SM'11) received the Laurea degree in communication engineering and the Ph.D. degree in information and communication theory from the Sapienza University of Rome, Rome, Italy, in 2001 and 2005, respectively. Since 2006, he has served as an Assistant Professor at the Department of Information, Electronics and Telecommunications Engineering, Sapienza University of Rome, where since 2015 he covers the position of Associate Professor. In 2010, he was a Visiting Assistant Professor with the Department of Electrical and Computer Engineering, University of British Columbia, Vancouver, BC, Canada. He was a Visiting Assistant Professor with the Department of Information Engineering of University of Padua in 2012. He is responsible for the international cooperation with colleagues in different countries and his research activities are in the field of visible light communications in the RGB-Comm Lab where he advises Ph.D. students and postdocs leading projects in the area of optical wireless. He is also responsible for the research activities in the field of underwater communications in the AMOUR-AQUALab for activities involving both acoustic and optical communications. He is author of more than 150 published works in the field of communication and signal processing. His research interests include MIMO systems, Internet of Things, underwater communications (acoustic and optical), Smart Grids, and Optical Wireless Systems, signal processing for communication. Regarding Optical Wireless, he organized several IEEE workshops and tracks in conferences. Prof. Biagi is currently a member of the IEEE Communications Society Technical Committee on Power Line Communications, Cybersecurity, and IEEE Communications Society Transmission Access on Optical Systems where he serves as secretary since 2021. He served as an Associate Editor for IEEE PHOTONICS TECHNOLOGY LETTERS and guest editor for IEEE Journal of SELECTED AREAS IN COMMUNICATIONS for a special issue entitled Localisation, Communication and Networking with VLC, 2018. Since 2021 he is Associate Editor of IEEE/OPTICA JOURNAL OF LIGHTWAVE TECHNOLOGY.